Enhancing Dam Infrastructure Safety through CFD-Based Spillway Assessment

Muhammad Hafiz Aslami[1], *Eldina* Fatimah[2,*], *Ikhlasul* Amal[3], *Davikia* Nastyakshan[4], *Cut Dwi* Refika[2], *Nina* Shaskia[2]

[1]Civil Engineering Department, Faculty of Engineering, Binus University, 11480, Indonesia
[2]Civil Engineering Department, Faculty of Engineering, Syiah Kuala University, 23111, Indonesia
[3]Master Program, Civil Engineering Department, Faculty of Engineering, Syiah Kuala University, 23111, Indonesia
[4] Bachelor Program, Civil Engineering Department, Faculty of Engineering, Syiah Kuala University, 23111, Indonesia

Abstract. Spillways play a crucial role in dam safety by controlling the release of excess floodwater. However, high discharge rates through these structures may lead to adverse hydraulic effects, such as cavitation and slug flow. This study examines these risks in the side spillway of the *Krueng Kluet* Dam, South Aceh, using a Computational Fluid Dynamics (CFD) approach. The model evaluates the flow conditions under operational discharges through velocity and pressure field simulations. The results indicate cavitation risk levels of 1 and 2—corresponding to no cavitation and potential cavitation—across most of the spillway. However, localized cavitation damage was detected near the downstream end of the chute at approximately 553 m and 580 m. These areas exhibited cavitation index values of 0.24 and 0.20, respectively. No signs of slug flow were observed in any section of the flow path. As a preventive measure, installing aerators or redesigning the chute with a stilling basin is proposed to reduce downstream flow velocity. This research provides design recommendations to improve spillway systems' hydraulic performance and safety and demonstrates the utility of CFD modelling for early identification of failure-prone zones.

1 Introduction

Flood events pose substantial hydrological and socio-economic challenges, particularly in regions with limited floodplain management and infrastructure capacity. In response to the floods, the Indonesian government initiated the development of the *Krueng Kluet* Dam, a multipurpose infrastructure in South Aceh Regency. The dam integrates several functions, including irrigation support, hydropower generation, aquaculture, tourism development, and flood regulation [1, 2]. Its presence is central to the region's water resource allocation and hydraulic safety strategies.

*Corresponding author: eldina.fatimah@usk.ac.id

The dam includes a side spillway comprising a crest, side channel, transition zone, and chute. This configuration is designed to safely convey excess discharge during peak hydrological conditions, ensuring the structural and operational reliability of the dam [3]. A physical hydraulic model of the structure was constructed at a scale of 1:60 to simulate the behavior of flow throughout the spillway system under various design discharges [4]. The results confirmed the overall functionality of the structure but indicated localized flow anomalies, particularly cavitation and transient surging, in the chute channel. To address these risks, design modifications were introduced, including changes in sill location, channel slope adjustment, and transition floor extension [4].

While physical modeling provides valuable insights into overall spillway performance, it remains limited in resolving localized pressure fluctuations and transient hydraulic responses. Accordingly, numerical methods such as Computational Fluid Dynamics (CFD) have been integrated into spillway assessments. Due to its mesh-free, Lagrangian framework, the Smoothed Particle Hydrodynamics (SPH) approach has demonstrated significant capability in simulating free-surface flows with complex geometries [5,6]. SPH enables the detailed prediction of velocity and pressure fields, making it suitable for assessing critical hydraulic phenomena that may compromise structural safety.

Cavitation remains a significant concern in high-velocity spillway flows. It arises when local static pressures fall below vapor pressure, forming vapor bubble and implosive collapse. This process can erode concrete surfaces and reduce structural durability [7]. Slug flow, which occurs in long chute channels, represents another risk as it creates unsteady surging regimes that impose uneven hydrodynamic forces and potential vibration effects [8,9]. Both phenomena underscore the need for predictive modeling and design interventions that minimize the likelihood of hydraulic instabilities.

In this context, the present study applies SPH-based CFD modeling to evaluate the hydraulic response of the *Krueng Kluet* Dam spillway under multiple discharge scenarios. The analysis emphasizes pressure distribution, velocity profiles, cavitation index, and flow regime stability. The findings are expected to provide refined insights into vulnerable sections of the spillway and support design improvements that strengthen dam safety under operational and extreme hydrological conditions.

2 Materials and methods

2.1 Smoothed Particle Hydrodynamics

Smoothed Particle Hydrodynamics (SPH) is one of the methods in numerical models, which is a particle-based numerical modeling method. SPH is a particle-type Lagrangian method with information in the form of position, velocity, pressure, and others, and then uses the particles to discretize the Navier-Stokes equations. After being discretized, the particles are considered weakly compressible (WCSPH), and particle updates are based on the interpolation of all particles in the characteristic length h [5]. 2D simulation forms particles in circles, while 3D is in the form of balls with characteristic lengths in the form of h according to simulation needs.

The law of conservation of continuum fluids has been changed from a partial differential form to one that is in accordance with particle-based simulations using integral equations based on interpolation functions that provide estimates of values at specific points. If a function *F(r)* in the domain *Ω* can be approached by an integral approach, such as Equation (1), (2), and (3), where *W* is the kernel function and *r* is the position vector [5].

$$F_{(r)} = \int_{\Omega} F_{(r')} W_{(r - r', h)} dr' \quad (1)$$

$$F(r_a) \approx \Sigma_b F(r_b)\, W(r_a - r_b, h)\, \Delta v_b \quad (2)$$

$$F(r_a) \approx \Sigma_b F(r_b)\, W(r_a - r_b, h)\, \left(\frac{m_b}{\rho_b}\right) \quad (3)$$

$$\frac{dv_a}{dt} = -\Sigma_b\, m_b \left(\frac{P_b + P_a}{\rho_b \cdot \rho_a} + \prod_{ab}\right) \nabla_a W_{ab} + g \quad (4)$$

The Equation above is the discrete procedure of the SPH method, and Figure 1 shows the particle approximation process of the SPH method. The calculation of particle i can be interpolated according to the surrounding particles in the domain. Therefore, Equation (3) can discretize the momentum conservation equation and obtain the discrete acceleration form in Equation (4).

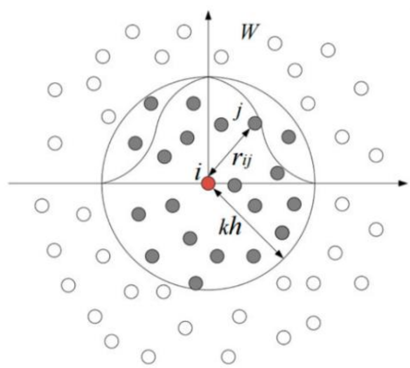

Fig. 1. The interpolation principle of the SPH method includes the kernel and particle approaches.

P is the pressure, v_a is particle a's velocity, ρ is the density, *m* is the particle's mass, *g* is the acceleration due to gravity (g = 9.8 m/s^2), ∏ and *ab* is the given artificial viscosity. Because the particle mass is the same, the fluid density calculation can only be obtained by discretizing the continuity equation through Equation (5).

$$\frac{d\rho_a}{dt} = \Sigma_b\, m_b\, v_{ab}\, \nabla_a W_{ab} \quad (5)$$

In the SPH method, which uses discrete solutions, fluid particles are generally assumed to have weak compressibility. Equation (4) and the Equation of state (5) determine the calculation of pressure particles. Therefore, Equation (6) can explain the calculation of pressure particles.

$$P = B\left[\left(\frac{\rho}{\rho_0}\right)^{\gamma} - 1\right] \quad (6)$$

Where $\gamma = 7$ for water, ρ_o = 1000 kg/m^3, $B = c^2_o\, \rho_o / \gamma$, and $c_o = c(\rho_o) = \sqrt{(\partial P/\partial \rho)}$ when $\rho = \rho_o$, c_o represents the speed of sound.

2.2 CFD Model Setup and Simulation Process

The numerical simulation of the spillway flow was carried out using the Smoothed Particle Hydrodynamics (SPH) method, implemented via the DualSPHysics platform. The kernel function applied in the simulation was the cubic spline or quintic Wendland, known for stability and interpolation accuracy [6].

The 3D spillway geometry was modelled with particles discretized using a particle spacing (Δp) determined based on the smallest geometric feature, as shown in Figure 2 [4,6]. Boundary conditions were defined with fixed-wall particles for structural interfaces, and inlet/outlet zones were adjusted for discharge control.

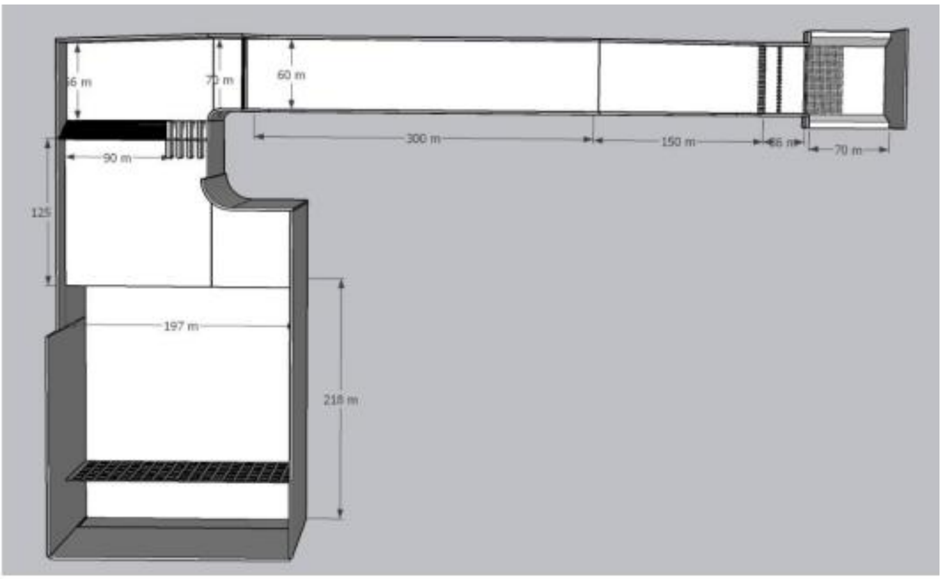

Fig. 2 3D Model Results of the Krueng Kluet Dam [6].

The simulation employed an artificial viscosity formulation based on Monaghan's model to stabilize high-gradient flows and suppress numerical noise. The inflow was based on the design discharge Q from dam planning documents, and the analysis focused on pressure and velocity distributions throughout the spillway, particularly to detect cavitation-prone zones [4,6].

2.3 Cavitation

Cavitation is a process related to surface damage to channel walls, pipes, and blades characterized by noise in a flow system [7]. Cavitation occurs when cavities or 'bubbles' of water vapor and other liberated gases form in flowing water. The flow may carry these to regions of higher pressure where they implode [7]. The occurrence of cavitation damage to a spillway can be predicted using the cavitation index. In this method, to prevent cavitation damage to a spillway, it is required to keep the flow cavitation index more than the cavitation inception index ($\sigma > \sigma_i$) everywhere on the structure.

$$\sigma = \frac{P - P_v}{\rho \frac{v^2}{2}} \tag{7}$$

$$P = P_a + P_g \tag{8}$$

Where σ is the cavitation inception index, P is reference flow pressure, P_a is atmospheric pressure, P_g is pressure on the surface of a structure, P_v is water vapor pressure, ρ is water density, and v is reference flow velocity. The value of the cavitation inception index is determined according to surface irregularities or surface roughness, and various equations have been presented based on research and experiments.

The cavitation damage level for a spillway has been predicted by two parameters: the flow velocity and cavitation index [8]. Five levels have been considered for cavitation damage risk to a spillway. The levels are presented based on the flow velocity and cavitation index (Table 1).

Table 1. Cavitation damage level.

Level	Cavitation damage risk	Intervals of velocity (m/s)	Intervals of cavitation index
1	No cavitation damage	$v \leq 5$	$\sigma > 1$
2	Possible cavitation damage	$5 < v \leq 16$	$0.45 < \sigma \leq 1$
3	Cavitation damage	$16 < v \leq 25$	$0.25 < \sigma \leq 0.45$
4	Serious damage	$25 < v \leq 40$	$0.17 < \sigma \leq 0.25$
5	Major damage	$v > 40$	$\sigma \leq 0.17$

2.4 Slug Flow

Slug flow is a hydraulic phenomenon that must be considered in constructing a chute channel structure. If this phenomenon occurs, it can cause uneven flow so that the resulting hydrodynamic force can endanger the stability of the construction. In addition, due to uneven flow, the flow velocity at the bottom of the chute channel becomes uneven, reducing damping effectiveness in the stilling basin [9].

If the design of the chute channel is more than 30.0 meters long, there is a danger of instability in the flow called slug flow. To control this risk, calculations need to be made with the Vendernikov number (V) and the Montuori number (M) in equations (8) and (9) [10].

$$\underline{V} = \frac{2bv}{3P\sqrt{gd\cos\theta}} \tag{8}$$

$$\underline{M}^2 = \frac{v^2}{gI\cos\theta} \tag{9}$$

Where b is the width of the channel base, v is the velocity, P is the wetted circumference (m), g is the acceleration of gravity (9.8 m/s^2), d is the average water depth, θ is the energy gradient angle, I is the average slope of the energy gradient, and L is the intended length.

After obtaining the calculated values of the Vendernikov and Montuori numbers, the next step is plotting these values on a graph representing the slug flow criteria, as shown in Figure 3. The graph provides a two-zone classification: the slug flow zone and the no slug flow zone. The diagonal line dividing these two regions serves as a boundary that indicates the critical condition at which the flow regime changes from stable to unstable.

This plotting method allows researchers to determine the flow regime by visually locating the calculated parameters on the graph. If the point falls within the zone of slug flow, it indicates the potential presence of unstable surging conditions, whereas a point located in the zone of no slug flow corresponds to a stable regime. The process transforms dimensionless numbers into a practical diagnostic tool that simplifies the evaluation of flow stability in hydraulic channels.

To support design analysis, several alternatives are commonly discussed in the literature for reducing the likelihood of slug flow [11]. These include adjustments to the channel cross-section, such as narrowing the width to regulate discharge distribution, or reducing the channel bed slope to decrease acceleration. Such considerations are integrated into the methodological framework to guide the assessment and control of slug flow phenomena in hydraulic structures.

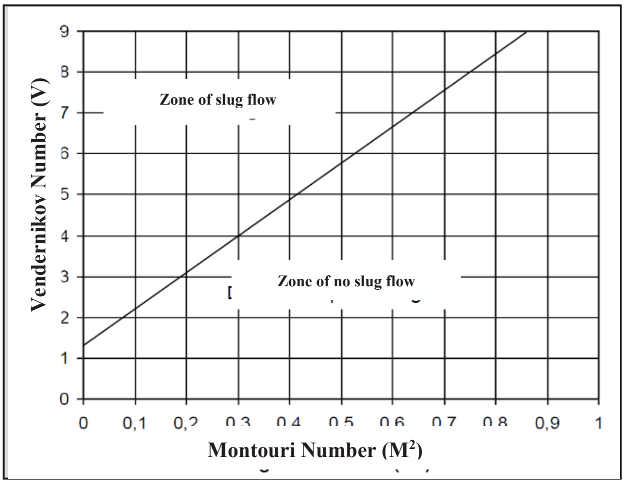

Fig. 3. Slug flow criteria graph [11].

3 Results

The numerical modeling of the *Krueng Kluet* Dam spillway was conducted and subsequently evaluated against analytical calculations for design return periods of Q_{50}, Q_{100}, and Q_{1000}, corresponding to discharge values of 1,210.78 m³/s, 1,495.66 m³/s, and 1,702.32 m³/s, respectively. The comparison focused on the root-mean-square (RMS) values derived from numerical simulations and analytical methods, as presented in Figure 4. To facilitate a consistent comparison, the RMS curves were normalized by the maximum values of the analytical data. The graphical representation illustrates that the RMS values from the numerical approach closely followed the analytical trends for all discharge scenarios, with discrepancies consistently below 10%.

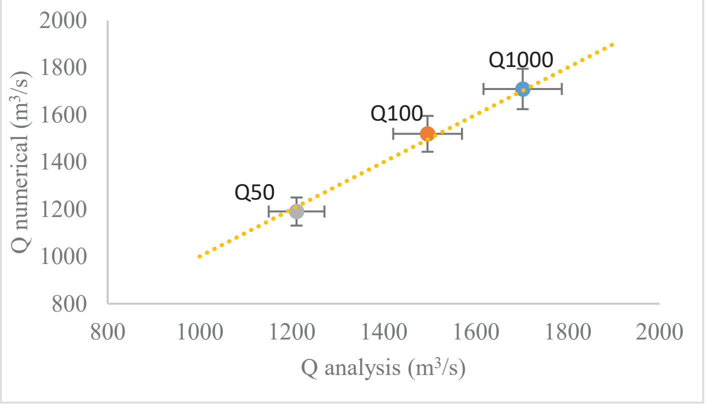

Fig. 4. RMS numerical and analysis results for discharge with 50, 100, and 1000 years return periods.

These results confirm that the numerical model provides a reliable representation of the hydraulic performance of the *Krueng Kluet* Dam spillway. The limited deviation indicates that the applied modeling framework successfully reproduces key flow characteristics and discharge capacities across flood scenarios. In particular, the close alignment with analytical predictions supports the robustness of the numerical approach in capturing flow dynamics under both moderate and extreme flood conditions. This agreement validates the computational method and provides confidence in extending the analysis toward more complex hydraulic phenomena, such as cavitation risk and flow regime stability, which are difficult to capture through purely analytical formulations.

Figure 5 presents the velocity field along the spillway components under the Q_{100} discharge condition (1,495.66 m³/s). At the crest (Figure 5a), flow velocities ranged between 3.0 and 6.0 m/s and remained uniformly distributed across the spillway width, demonstrating effective crest regulation. In the side channel (Figure 5b), the velocity increased progressively from less than 5.0 m/s near the inlet to 12.0–15.0 m/s downstream, consistent with geometric convergence and gravitational acceleration.

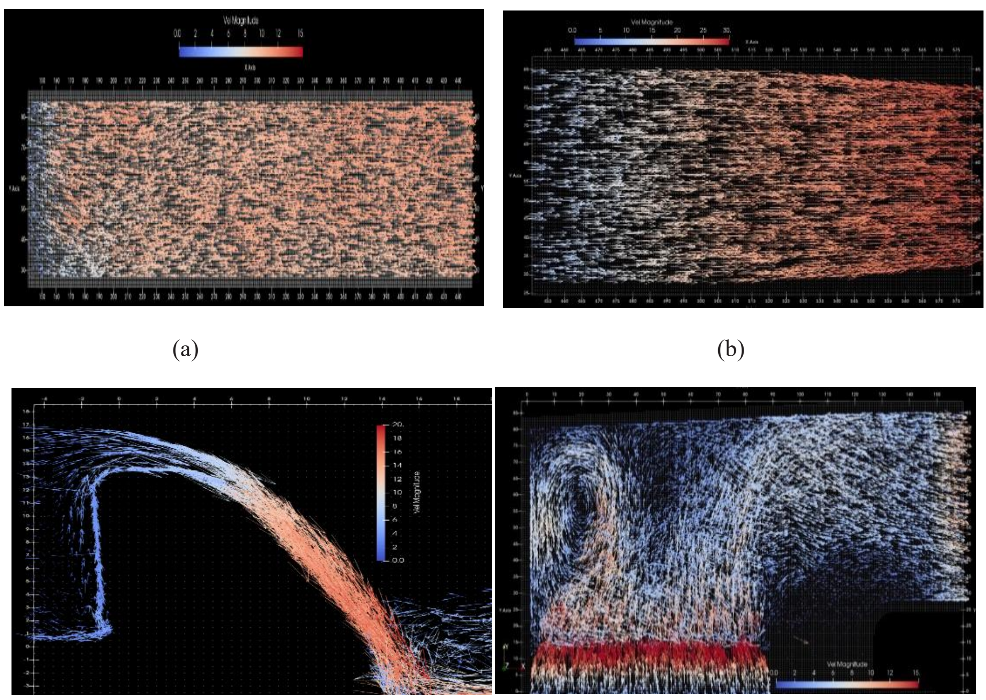

(a) (b) (c) (d)

Fig. 5. Flow pattern through (a) crest of spillway, (b) side channel, (c) transition channel, and (d) chute channel for Q_{100}.

The transition channel (Figure 5c) exhibited the highest velocity gradients, with peak velocities exceeding 15.0 m/s. These rapid accelerations and slope variations correspond to localized pressure drops, in line with cavitation indices of 0.24 and 0.20 observed at 553 m and 580 m. This confirms that the transition–chute section is the most critical zone concerning cavitation risk. Finally, the chute and stilling basin (Figure 5d) displayed jet velocities of 15.0–20.0 m/s entering the basin, followed by large vortices and recirculation zones with velocities below 5 m/s. This significant energy dissipation indicates that the stilling basin effectively stabilizes downstream conditions and reduces erosion risk.

Cavitation index analysis requires pressure and flow velocity data. The recapitulation of the cavitation index calculation can be seen in Table 2. Based on the results of the analysis that has been carried out, it was found that the cavitation index value is at risk level 1 and 2, where the building does not or is likely to experience cavitation damage. A solution for cavitation hazards at risk level 2, requiring surface treatment, such as applying cement to the surface, and smoothing the channel surface [12].

Table 2. Recapitulation of index cavitation on the spillway.

Distance (m)	Structure	Q_{50}	Q_{100}	Q_{1000}	Distance (m)	Structure	Q_{50}	Q_{100}	Q_{1000}
0,52	Crest of spillway	51,5	11,8	8,8	296,80	Transition channel	15,4	2,7	1,9
1,56		50,4	12,5	8,9	328,30		17,6	4,2	2,0
3,06		9,9	9,7	6,6	354,10		8,4	2,0	1,7
4,26		3,7	9,2	7,9	383,80		15,0	3,7	1,8
5,80		2,3	1,6	2,0	409,60		10,2	6,2	1,9
7,15		4,7	1,3	2,4	421,30		9,8	7,5	1,7
8,40		2,4	1,9	2,1	433,30		19,5	3,4	1,9
9,80		1,8	1,7	1,3	439,00		16,8	3,4	1,7
11,15		1,3	1,6	2,6	441,40		9,9	2,9	1,7
12,35		1,9	2,4	3,8	444,70		15,2	3,4	1,7
13,45		12,1	9,1	11,8	454,20	Chute channel	6,8	6,5	1,4
10,92	Side channel	39,6	32,0	28,3	463,90		6,9	6,5	1,2
44,88		71,4	68,5	16,7	475,00		5,9	3,0	0,8
78,60		92,5	9,6	6,9	486,40		2,0	2,2	0,7
107,25		83,7	59,7	24,9	503,40		1,4	1,1	0,5
149,50	Transition channel	57,3	7,9	3,2	519,80		1,2	0,7	0,3
174,10		19,6	3,4	2,5	536,50		0,6	0,3	0,3
193,60		16,6	4,3	2,4	553,10		1,0	0,4	0,2
220,90		16,6	2,7	2,3	565,30		1,1	0,5	0,3
245,50		18,3	3,2	2,2	579,70		1,4	0,9	0,2
276,40		23,3	3,0	2,5					

Based on the results presented in Table 2, cavitation was observed at the downstream end of the chute channel under the Q_{1000} discharge condition, specifically at distances of 553m and 580 m. The cavitation index values at these locations were 0.24 and 0.20, respectively, indicating a Level 3 cavitation risk. Mitigation measures are necessary to minimize structural damage when cavitation is detected in a spillway channel [12]. Recommended interventions include installing aerators or modifying the stilling basin to reduce velocity at the chute toe by generating controlled backflow.

The occurrence of cavitation at these locations is closely associated with abrupt changes in channel slope and rapid flow acceleration, which produce localized pressure drops below the vapor pressure of water. These hydraulic and geometric discontinuities create favorable conditions for vapor bubble formation and subsequent collapse. The implosive collapse of these bubbles can result in localized erosion and surface deterioration, posing long-term risks to the structural integrity of the spillway.

In addition to cavitation, the potential for slug flow was assessed using the Vendernikov and Montuori numbers. This evaluation required data on mean flow depth and velocity in the side, transition, and chute channels. The energy loss (H_f) and flow angle (ϴ) were calculated from these values to characterize flow conditions. The computed Vendernikov and Montuori numbers were plotted, as shown in Figure 6, to determine whether the results fell within the slug flow or no-slug-flow zones. The findings demonstrated that all side, transition, and chute channel points fell within the no-slug-flow zone, confirming hydraulic stability against surging flow conditions.

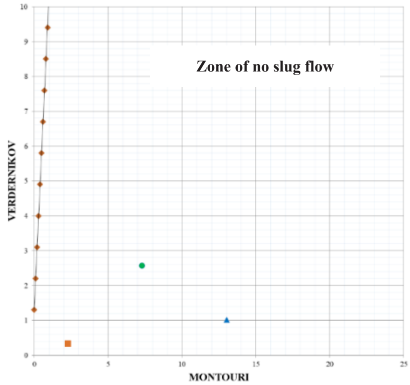

(a)

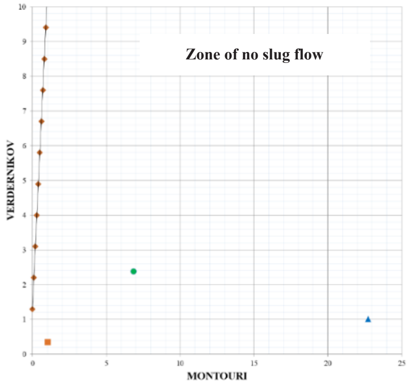

(b)

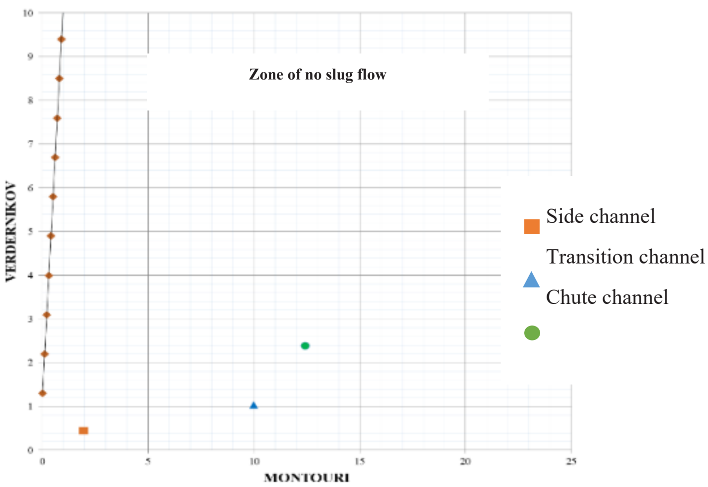

(c)

Fig. 6. Slug flow analysis graph for (a) Q_{50}, (b) Q_{100}, and (c) Q_{1000}.

The side channel recorded Montuori and Vendernikov numbers of approximately 0.35 and 11.5, respectively, placing it firmly in the no-slug-flow zone and reflecting deep, uniform flow. The Montuori number in the transition channel increased to about 4.8, while the Vendernikov number decreased to around 3.2, indicating accelerated but stable flow. The chute channel exhibited the highest Montuori value of about 12.5 with a corresponding Vendernikov number near 2.3, characteristic of high-velocity jet flow. Despite these variations, all calculated points remain within the no-slug-flow zone.

This progression—from high V and low M^2 in the side channel to low V and high M^2 in the chute—corresponds to the expected hydraulic behavior of a side spillway system. Previous studies have documented similar trends: Rajaratnam [13] and Khatsuria [14]. They emphasized that properly designed transition and chute geometries prevent slug flow formation. At the same time, Wibowo and Dermawan [15] demonstrated through numerical modeling of a side spillway that CFD analysis provides reliable predictions of flow regime stability. The alignment of the present results with these validated studies underscores the accuracy of the numerical modeling approach in characterizing flow regime transitions in the Krueng Kluet Dam spillway.

4 Conclusion

This study employed CFD-based numerical modeling to assess cavitation and slug flow risks in the Krueng Kluet Dam side spillway. The results show that most spillway sections remain at cavitation risk levels 1–2. However, at the downstream chute under Q_{1000}, cavitation risk level 3 was identified at 553 m and 580 m with index values of 0.24 and 0.20, requiring mitigation such as aerators or a sinking-basin stilling basin to reduce flow velocity. In contrast, slug flow analysis using Vendernikov and Montuori numbers confirmed that the side channel, transition, and chute lie within the no-slug-flow zone, demonstrating hydraulic stability. These findings validate the effectiveness of CFD modeling in identifying localized risks and provide a basis for targeted design improvements to enhance spillway safety and dam reliability.

References

1. D. C. Froehlich and D. G. Diaz, Dam Safety—Living with the Risk of Failure. A Syst. Eng. Approach to Disaster Resilience. Lect. Notes Civ. Eng. **205** (2022). https://doi.org/10.1007/978-981-16-7397-9_30
2. V. Variadi, K. Iqbal, F. Mufti, and R. Adriman, Keureuto Dam Operation for Flood Control System. E3S Web Conf. **476**, 01049 (2024). https://doi.org/10.1051/e3sconf/202447601049
3. Q. Aini, E. Fatimah, and A. Azmeri, Kajian Panjang Loncatan Hidrolik Pada Model Fisik Kolam Olak Bendungan Krueng Kluet Kabupaten Aceh Selatan. Teras J. **12**, 1, pp. 81–92 (2022). http://dx.doi.org/10.29103/tj.v12i1.619
4. S. Kamal, Cavity and Slug Flow on The Physical Model Chutes Channel of Krueng Kluet Dam, South Aceh Regency, Bachelor's Thesis, Syiah Kuala Univ, Banda Aceh, Faculty of Engineering (2021).
5. A. Trimulyono, H. Hashimoto, and A. Matsuda, Experimental Validation of Single- and Two-Phase Smoothed Particle Hydrodynamics on Sloshing in a Prismatic Tank. J. Mar. Sci. Eng. 7, 8, 247 (2019). https://doi.org/10.3390/jmse7080247.
6. Amal, Hydraulic Modeling of Krueng Kluet Dam, South Aceh Regency Using Computational Fluid Dynamic, Master Thesis, Syiah Kuala Univ, Banda Aceh, Faculty of Engineering (2024).
7. Y. Sutopo, Kavitasi di Dasar Saluran Curam, (Andi, Yogyakarta 2014).
8. E. F. Kermani, G. A. Barani, and M. Ghaeini-Hessaroeyeh, Investigation of Cavitation Damage Levels on Spillways. World Appl. Sci. J. **12**, 1, pp. 73–78 (2013). https://doi.org/10.5829/idosi.wasj.2013.21.1.2630
9. C. Wibowo, V. Dermawan, and P. T. Juwono, Pemodelan Numerik Pelimpah Samping Waduk Telagawaja Bali Kabupaten Karangasem Dengan Analisa Komputasi Fluida Dinamis. J. Tek. Pengairan. Univ. Brawijaya, Malang. **7**, 2, pp. 184-192 (2016). Available at:

https://jurnalpengairan.ub.ac.id/index.php/jtp/article/view/294
10. Departemen Pekerjaan Umum, Standar Perencanaan Bangunan Utama (KP-02), (Galang Persada, Jakarta, 2013).
11. C. A. Sulistiono, Kajian Hidraulika Pelimpah Samping Bendungan Raknamo Kupang NTT dengan Uji Model Fisik 1:50, Bachelor's Thesis, Universitas Brawijaya, Malang, Faculty of Engineering (2016).
12. J. A. Kells and C. D. Smith, Reduction of cavitation on spillways by induced air entrainment. Can. J. Civ. Eng. **18**, 3, pp. 358–377 (1991). https://doi.org/10.1139/l91-047
13. Rajaratnam, N. (1990). *Skimming flow in side-weir channels*. *Journal of Hydraulic Research*, 28(4), 477–493. https://doi.org/10.1080/00221689009499904
14. Khatsuria, R. M. (2005). *Hydraulics of Spillways and Energy Dissipators*. CRC Press, Taylor & Francis Group. https://doi.org/10.1201/9780203020593
15. Wibowo, A. C., & Dermawan, V. (2016). *Pemodelan numerik pelimpah samping Waduk Telagawaja Bali Kabupaten Karangasem dengan analisa komputasi fluida dinamis*. *Jurnal Teknik Pengairan (JTP)*, 7(2), 126–136. https://jurnalpengairan.ub.ac.id/index.php/jtp/article/view/294